Marine Genomics 48 (2019) 100692

Contents lists available at ScienceDirect

Marine Genomics

journal homepage: www.elsevier.com/locate/margen

Method paper

Transcriptional profiles of early stage red sea urchins (*Mesocentrotus franciscanus*) reveal differential regulation of gene expression across development

Juliet M. Wong[a,*], Juan D. Gaitán-Espitia[b], Gretchen E. Hofmann[a]

[a] Department of Ecology, Evolution and Marine Biology, University of California Santa Barbara, Santa Barbara, CA 93106, USA
[b] The Swire Institute of Marine Science, School of Biological Sciences, The University of Hong Kong, Pokfulam Road, Hong Kong Special Administrative Region

ARTICLE INFO

Keywords:
Red sea urchin
Mesocentrotus franciscanus
RNA-seq
De novo assembly
Early development

ABSTRACT

The red sea urchin, *Mesocentrotus franciscanus*, is an ecologically important kelp forest species that also serves as a valuable fisheries resource. In this study, we have assembled and annotated a developmental transcriptome for *M. franciscanus* that represents eggs and six stages of early development (8- to 16-cell, morula, hatched blastula, early gastrula, prism and early pluteus). Characterization of the transcriptome revealed distinct patterns of gene expression that corresponded to major developmental and morphological processes. In addition, the period during which maternally-controlled transcription was terminated and the zygotic genome was activated, the maternal-to-zygotic transition (MZT), was found to begin during early cleavage and persist through the hatched blastula stage, an observation that is similar to the timing of the MZT in other sea urchin species. The presented developmental transcriptome will serve as a useful resource for investigating, in both an ecological and fisheries context, how the early developmental stages of this species respond to environmental stressors.

1. Introduction

The red sea urchin *Mesocentrotus franciscanus* (A. Agassiz, 1863) is found along the West Coast of North America, ranging from Baja California, Mexico to Kodiak, Alaska, USA (Ebert et al., 1999). *M. franciscanus* is harvested for its gonads (i.e., roe), and in recent decades has suffered overfishing and exploitation as a high-demand wild fishery species (Andrew et al., 2002; Keesing and Hall, 1998). In terms of worth, the export value of roe in the United States was estimated to be approximately $28.7 million in 2011 (Rogers-Bennett, 2013). However, the price of red sea urchins harvested in the states of California, Oregon, and Washington has risen in recent years, increasing from $0.70 USD per pound in 2011 to $1.73 USD per pound in 2018 according to data reported by the Pacific Fisheries Information Network (PacFIN) (www.pacfin.psmfc.org; accessed 5 April 2019).

As a valuable wild fishery, red sea urchins are found in temperate rocky reefs in nearshore coastal regions. As benthic marine invertebrates in coastal marine ecosystems, they are threatened by ocean change (Sato et al., 2018), including future ocean acidification in regions dominated by episodic upwelling (Chan et al., 2017) and from marine heat waves (Gentemann et al., 2017). For example, between 2013 and 2016, anomalous warming events associated with "the Blob" led to dramatically increased sea surface temperatures in the northeast Pacific Ocean (Bond et al., 2015; Gentemann et al., 2017; Hu et al., 2017). While a direct cause-effect relationship between these warming events and red urchin harvests has not been formally established, in California alone, the weight of harvested *M. franciscanus* decreased from 6320 to 2669 metric tons per year between 2013 and 2016 (www.pacfin.psmfc.org; accessed 5 April 2019). Importantly, marine heat waves like "the Blob" are predicted to increase in frequency and intensity in the future (Oliver et al., 2018); these events will likely have an impact on marine systems, including organism physiology, species abundances, and population biogeographic distributions (Frölicher and Laufkötter, 2018; Leung et al., 2017; Sanford et al., 2019). Ecologically, *M. franciscanus* acts as an important ecosystem engineer by controlling algae populations, particularly in kelp forest ecosystems, and are capable of transforming algal communities into urchin barrens (Leighton et al., 1966; Rogers-Bennett, 2007). Given the high economic and ecological importance of *M. franciscanus*, as well as its potential vulnerability to environmental change, genomic resources are very useful for studying and monitoring this species.

The introduction of next-generation sequencing and increasing affordability of associated technologies has expanded the molecular resources and knowledge available for non-model species, particularly

* Corresponding author.
E-mail addresses: julietmwong@ucsb.edu (J.M. Wong), jdgaitan@hku.hk (J.D. Gaitán-Espitia), hofmann@ucsb.edu (G.E. Hofmann).

https://doi.org/10.1016/j.margen.2019.05.007
Received 26 April 2019; Received in revised form 28 May 2019; Accepted 29 May 2019
Available online 19 June 2019
1874-7787/ © 2019 Elsevier B.V. All rights reserved.

those of high value to fisheries and aquaculture. Annotated and assembled *de novo* transcriptomes have been published across a variety of valuable fishery and aquaculture species, including mollusks (Coppe et al., 2012; De Wit and Palumbi, 2012; Tian et al., 2018; Zhao et al., 2012), crustaceans (Ghaffari et al., 2014; Lv et al., 2014; Souza et al., 2018), echinoderms (Gaitán-Espitia et al., 2016; Gillard et al., 2014; Jo et al., 2016), and fishes (Carruthers et al., 2018; Ji et al., 2012; Liao et al., 2013). These transcriptomes are useful for investigating parameters important to fisheries health and management, such as population dynamics, evolutionary processes, the effects of abiotic stress, disease susceptibility and resilience, and stock assessments (Valenzuela-Quiñonez, 2016; Wenne et al., 2007). For example, assembled transcriptomes have been used to investigate salinity stress in the Pacific oyster *Crassostrea gigas* (Zhao et al., 2012), and viral infection in the Pacific whiteleg shrimp *Litopenaeus vannamei* (Chen et al., 2013). Transcriptomic data have also been used to investigate patterns of gene flow and local adaptation in the red abalone *Haliotis rufescens* (De Wit and Palumbi, 2012). Here, we used RNA sequencing (RNA-seq) to assemble and annotate a developmental transcriptome for the economically and ecologically important sea urchin, *M. franciscanus*, and assessed patterns of gene expression throughout early development. This tool could be used to assess the response of early stages to climate-changed related stressors.

Numerous studies have used transcriptomics to investigate how marine organisms respond to changes in their environment that are related to climate change, such as elevated temperatures and lowered pH and oxygen concentrations (Ekblom and Galindo, 2011; Franks and Hoffmann, 2012; Reusch and Wood, 2007). Describing the transcriptional dynamics of *M. franciscanus* during its early development is particularly pertinent, as the early stages of development are believed to be the most vulnerable times during the life history of many marine organisms (Byrne, 2011; Dupont and Thorndyke, 2009; Gosselin and Qian, 1997; Kurihara, 2008). A reduction in fitness at the embryological and larval stages leading to poor recruitment could have devastating impacts on marine population dynamics. As rapid environmental change continues, the early life stages may act as a bottleneck that dictates whether a species will be successful in the future (Byrne, 2012; Byrne and Przeslawski, 2013; Kurihara, 2008).

Several recent studies have reported developmental transcriptomes for marine invertebrates (Brekhman et al., 2015; Gildor et al., 2016; Heyland et al., 2011; Lenz et al., 2014; Zeng et al., 2011), and have described stage-specific expression of many transcription factors. Such transcriptomes help to identify which genes are important for development as well as the timing of expression of these genes. One group of processes that occur during development involves the change of control from the maternal to the zygotic genome, identified as the maternal-to-zygotic transition (MZT), when there is a shift in expression from maternal to zygotic transcripts (Shier, 2007; Tadros and Lipshitz, 2009). Understanding the timing of the MZT is important for interpreting expression dynamics during early development. In general, the generation and characterization of developmental transcriptomes provide useful genomic resources that offer the opportunity to unveil mechanisms underlying developmental plasticity and its role in buffering different abiotic stressors across ontogeny.

Here, we present a developmental transcriptome for *M. franciscanus* that represents eggs as well as embryos and larvae from six stages of development: 8- to 16-cell, morula (composed of approximately 64 cells), hatched blastula, early gastrula, prism, and early pluteus. The developmental transcriptome presented here will provide insight into the timing of the MZT and will help identify genes and regulatory pathways that are important for successful development at each stage. Overall, this is an important resource for transcriptomic analyses of this species, including ecological or fisheries studies that use gene expression to assess the response of early developmental stages to stress.

2. Materials and methods

2.1. Animal collection and culturing

Adult sea urchins were collected in May 2016 at Mohawk Reef, CA, USA (34° 23.606′ N, 199° 43.807′ W) under California Scientific Collection permit SC-1223. Urchins were immediately transported to the Marine Science Institute at the University of California, Santa Barbara (UCSB) (Santa Barbara, CA), and maintained in flow-through seawater tanks for approximately 1 week prior to spawning. Spawning was induced via intracoelomic injection of 0.53 M KCl. Egg samples (EG) were collected by gently transferring ~5000 eggs into a 1.5 mL microcentrifuge tube, quickly pelleting the sample by centrifugation, removing the excess seawater, and flash freezing the sample using liquid nitrogen. All samples were stored at −80 °C. Test fertilizations were performed to verify egg-sperm compatibility. The eggs from two females were gently pooled together and were fertilized using sperm from a single male. To avoid polyspermy, dilute sperm was slowly added to the eggs until at least 95% fertilization success was reached. The newly fertilized embryos were then placed into each of three replicate culture vessels (total volume = 12 L) at a concentration of ~9 embryos per mL of seawater.

All *M. franciscanus* early developmental stage (EDS) cultures were raised in 0.35 µm filtered, UV-sterilized seawater (FSW). The EDS cultures were raised at ~15 °C and ~425 µatm pCO_2. These conditions were chosen to represent average, "normal" ambient abiotic conditions that populations of *M. fransciscanus* have been observed to experience *in situ* near Mohawk reef; these observations are made via sensor arrays deployed by the Santa Barbara Coastal LTER (Hofmann and Washburn, 2015). During the EDS culturing, water temperature was controlled using a Delta Star® heat pump with a Nema 4× digital temperature controller (AquaLogic, San Diego, CA, USA), which maintained culturing temperatures at 15 °C. A flow-through CO_2-mixing system modified from Fangue et al. (2010) was used to ensure stable carbonate chemistry conditions throughout development. The CO_2 system was used to establish a 5-gal reservoir tank, in which water was treated to the target pCO_2 level prior to delivering the treated water to each culture vessel.

Each culture vessel was composed of two, nested 5-gal buckets (12 L capacity). The inner bucket had a dozen holes 5.5 cm in diameter, each fitted with 64-µm mesh to prevent the loss of embryos or larvae while allowing for a flow-through of seawater. Seawater flow to each vessel was controlled using irrigation button drippers (DIG Corporation), which regulated the flow to a rate of 4 L/h. Each vessel contained a 15 cm × 15 cm plastic paddle driven by a 12-V motor to allow for continuous, gentle mixing and to prevent early embryos from settling to the bottom of the bucket.

Embryos and larvae were sampled at six developmental stages: 8- to 16- cell (CL; ~4 h post-fertilization (hpf)), morula (MO; ~7 hpf), hatched blastula (BL; ~16 hpf), early gastrula (GA; ~29 hpf), prism (PR; ~44 hpf), and early pluteus (PL; ~64 hpf). While the development of *M. franciscanus* in culture is generally synchronous, during early cellular divisions, it is unlikely to collect a large batch of embryos that are exhibiting identical timing. As such, the samples collected at the 8- to 16-cell stage (CL) were composed of a mixture of embryos undergoing their third and fourth cleavage divisions. At the morula stage (MO), all embryos were composed of approximately 64 or more cells. The blastula stage (BL) was designated by the enzymatic digestion of the fertilization envelope and emergence of swimming blastula. The early gastrula (GA) stage was designated by the formation of mesenchyme cells and an archenteron extended to approximately one-half the body length. The prism stage (PR) was identified by the formation of the pyramid-like prism shape, the archenteron becoming tripartite, and the early development of skeletal rods. Lastly, the early pluteus state (PL) was defined as having internal structures, including the mouth, esophagus, stomach and anus, as well as anterolateral and postoral skeletal

body rods and the early formation of feeding arms. Samples from each of the three culture vessels were taken at each developmental stage. All samples were preserved using the same methods for preserving the eggs.

Temperature, salinity, pH, and total alkalinity (TA) were recorded daily to monitor the culturing conditions throughout development. Temperature was measured using a wire thermocouple (Thermolyne PM 20700/Series 1218), and salinity was measured using a conductivity meter (YSI 3100). Daily pH measurements were conducted by following the standard operating procedure (SOP) 6b (Dickson et al., 2007a, 2007b), using a spectrophotometer (Bio Spec-1601, Shimadzu) and *m*-cresol purple (Sigma-Aldrich) indicator dye. Water samples for TA were poisoned with saturated 0.02% mercuric chloride. TA was estimated using SOP 3b (Dickson et al., 2007a,b). Using the carbonic acid dissociation constants from Mehrbach et al. (1973) refit by Dickson and Millero (1987), parameters of pCO_2, Ω_{ara}, and Ω_{cal} were calculated using CO_2calc (Robbins et al., 2010).

2.2. RNA extractions and sequencing

Total RNA was extracted using 500 μL of Trizol® reagent, following the manufacturer's instructions (Invitrogen). Briefly, each sample was homogenized in Trizol® reagent by passing the sample three times through decreasing sizes of needles (21-guage, 23-gauge, and then 25-gauge). A chloroform addition and centrifugation were used to isolate the RNA-containing upper aqueous phase. The RNA was precipitated in isopropyl alcohol, washed using ethanol, and resuspended in DEPC-treated water. RNA purity, quantity, and quality were verified using a NanoDrop® ND100, a Qubit® fluorometer, and a Tapestation 2200 system (Agilent Technologies).

Three libraries were generated from triplicate samples of eggs. For each developmental stage, one library was generated for each of the three replicate culture vessels. This resulted in a total of 21 libraries. Libraries were generated using high quality total RNA (RIN values > 9.1) using a TruSeq Stranded mRNA Library Preparation Kit (Illumina) following the manufacturer's instructions. The quantity and quality of each library were verified using a Qubit® fluorometer and a Tapestation 2200 system (Agilent). The libraries were submitted to the Genome Center at the University of California, Davis for sequencing on an Illumina HiSeq 4000 sequencer on two lanes with 150 base-pair (bp) paired-end reads.

2.3. De novo transcriptome assembly

Additional *M. franciscanus* raw sequence data from Gaitán-Espitia and Hofmann (2017) were included with sequence data from our 21 libraries to generate the *de novo* transcriptome. These data represented gastrula stage embryos (GenBank accession numbers SRS823202 and SRS823216) and pluteus larvae (accession numbers SRS823218 and SRS82322) of Bioproject PRJNA272924. Any potential adapter sequence contamination as well as any base pairs with quality scores below 30 were removed from all raw sequence data using Trim Galore! (version 0.4.1) (Krueger, 2015). Sequence quality was verified using FastQC (version 0.11.5) (Andrews, 2010).

The transcriptome was assembled following a pipeline available from the National Center for Genome Analysis Support (NCGAS) at Indiana University (https://github.com/NCGAS/de-novo-transcriptome-assembly-pipeline). This workflow generates a combined *de novo* assembly that uses multiple assemblers with multiple parameters. Prior to assembly, the data were normalized using the *in silico* read normalization function in Trinity (version 2.6.6) (Grabherr et al., 2011). Multiple *de novo* assemblies were created using different assemblers with different selections of kmer lengths: Trinity (version 2.6.6) (kmer = 25), SOAPdenovo-Trans (version 1.03) (Xie et al., 2014) (kmers = 35, 45, 55, 65, 75, and 85), Velvet (version 1.2.10) (Zerbino and Birney, 2008) and Oases (version 0.2.09) (Schulz et al., 2012) (kmers = 35, 45, 55, 65, 75, and 85), and Trans-ABySS (version 2.0.1) (Robertson et al., 2010) (kmers = 35, 45, 55, 65, 75, and 85). These 19 assemblies were then combined using EvidentialGene (version 2013.07.27) (Gilbert, 2013), which removes perfect redundancy and fragments to reduce false transcripts while predicting unique transcripts within the final assembly. Quast (version 5.0.0) (Gurevich et al., 2013) was used to generate basic quality metrics of the final assembly. BUSCO (version 3.0.2) (Simão et al., 2015) was used to assess completeness of the final assembly using the single-copy ortholog reference for metazoans.

2.4. Gene prediction and functional annotation

Gene models from the *de novo* assembled transcriptome were inferred and annotated using the BLASTP (against the nr database), BLASTN (against the eukaryotic nt database) and BLASTX (against the Uniprot database, Swiss-Prot and TrEMBL) algorithms with an e-value cutoff of $1e^{-5}$. Annotated sequences were further searched for Gene Ontology (GO) terms using Blast2GO software (version 5.2.5) according to the main categories of Gene Ontology (GO; molecular functions, biological processes and cellular components) (Ashburner et al., 2000). Complementary annotations were done with the InterProScan v.5 software (Jones et al., 2014). Finally, the annotation results were further fine-tuned with the Annex and GO slim functions and the enzyme code annotation tool of the Kyoto Encyclopedia of Genes and Genomes (KEGG) (Kanehisa and Goto, 2000) implemented in Blast2GO.

2.5. Expression quantitation and differential expression analyses

Trimmed sequence data from the 21 libraries were mapped onto the *de novo* reference transcriptome and expression values were calculated using RSEM (version 1.3.0) (Li and Dewey, 2011) and bowtie2 (version 2.3.2) (Langmead and Salzberg, 2012). Using the LIMMA package (Ritchie et al., 2015) in R (version 3.4.4), the data were filtered to sequences that have > 0.5 counts per million mapped reads across at least three of the 21 samples. A trimmed mean of M-values (TMM) normalization method (Robinson and Oshlack, 2010) was used to apply scale normalization to the read counts. The data were voom-transformed using LIMMA to convert the read counts to log-counts per million while accounting for sample-specific quality weights and blocking design (i.e., technical replicates). The filtered, normalized and voom-transformed data were used to perform a principal component analysis (PCA) using the prcomp function in R. An unweighted pair group method with arithmetic mean (UPGMA) method using Euclidean distances was implemented to perform hierarchical clustering on the principal components using the HCPC function of the FactoMineR package (Le et al., 2008) in R.

Using the WGCNA package (Langfelder and Horvath, 2008) in R, a Weighted Gene Co-Expression Network Analysis (WGCNA) was performed on the same filtered, normalized and voom-transformed data to identify clusters of similarly expressed genes into modules, in which each module contained a minimum of 30 genes. Modules with highly correlated eigengenes were merged using a threshold of 0.27 (i.e., a height cut-off of 0.27 and a correlation of 0.73 for merging). Eigengene expression was correlated with eggs and each developmental stage (i.e., EG, CL, MO, BL, GA, PR, and PL), and a heatmap was generated to visualize significant correlations between each stage and module.

Functional enrichment analyses were performed on lists of genes within modules with significant correlations to a developmental stage (r^2 correlation ≥ 0.50 and p-value $\leq .05$). Enrichment analyses were performed in Blast2GO (version 5.2.5) using a Fisher's Exact Test with an FDR filter value of 0.05 to identify gene ontology (GO) terms within the GO categories: biological process, molecular function, and cellular component.

Table 1
Transcripts that play a functional role during the MZT.

Transcript ID	Name	Description
058424	*dgcr8*	Microprocessor complex subunit DGCR8-like
103747	*dicer*	Endoribonuclease Dicer
035070	*smaug1*	Protein Smaug homolog 1 isoform X1
089348	*smg7*	Protein SMG7 isoform X2
052093	*smg8*	Protein smg8
035665	*smg9*	Protein SMG9-like
089934	*alx*	Aristaless-like homeobox protein
082528	*bra*	Transcription factor Brachyury
015822	*dri*	Protein dead ringer homolog
036581	*gcm*	Glial cells missing transcription factor
035045	*gsc*	Homeobox protein goosecoid-like
047087	*hox11/13b*	Transcription factor Hox11/13b
104463	*lefty2*	Left-right determination factor 2-like
047266	*nodal*	Nodal homolog 2-A-like
076942	*wnt8*	Wnt8

2.6. Survey of the maternal-to-zygotic transition

To investigate the timing of the maternal-to-zygotic transition (MZT), two aspects of the data were probed: (1) the loss of maternally-derived transcripts, and (2) the initiation of zygotic transcription. To examine the loss of maternally-derived transcripts, putative genes related to the removal of maternal RNAs were identified. These included putative genes for the *microprocessor complex subunit DGCR8* (*dgcr8*), *endoribonuclease dicer* (*dicer*), *smaug* (*smaug1*), and *nonsense mediated mRNA decay* (*smg7*, *smg8*, and *smg9*) (Gildor et al., 2016; Marlow, 2010; Tadros and Lipshitz, 2009) (Table 1). The expression levels of these transcripts were examined across the eggs and early development. Additionally, a heatmap was constructed using Euclidean distances to visualize the expression of maternal transcripts throughout development. Transcripts expressed in the eggs were considered to be maternal. The heatmap was constructed using the top 500 transcripts expressed in unfertilized eggs (EG).

To examine the initiation of zygotic transcription, transcripts associated with zygotic development were targeted. Putative genes for *aristaless-like homeobox* (*alx*), *brachyury* (*bra*), *dead ringer* (*dri*), *glial cells missing* (*gcm*), *goosecoid* (*gsc*), *homeobox 11/13b (hox11/13b)*, *left-right determination factor 2* (*lefty2*), *nodal*, and *wnt8* were targeted within *M. franciscanus* (Tadros and Lipshitz, 2009; Wei et al., 2006) (Table 1). The expression levels of these transcripts were examined in eggs and as early development progressed. A heatmap was also constructed using Euclidean distances to visualize the expression of transcripts that were not maternally expressed (i.e., not expressed in unfertilized eggs). Transcripts with a negative expression value of $\log_2$ counts per million reads ($\log_2$ CPM < 0) at the EG stage were selected, for a total of 19,044 transcripts. Using these transcripts, a heatmap was constructed to visualize at what stages throughout development these transcripts were expressed.

3. Results and discussion

3.1. Culturing conditions

The embryo and larval cultures developed normally with little to no mortality observed throughout development. Temperature and seawater chemistry conditions were stable throughout the ~64 hour culturing period. Across all replicate culture vessels, the temperature was 15.3 ± 0.1 °C, the salinity was 33.4 ± 0.04, the pH was 8.00 ± 0.03, the pCO_2 level was 438 ± 33.1 μatm, and the TA was 2228.97 ± 3.19 μmol kg^{-1}.

Table 2
Statistics of *de novo* transcriptome assembly.

Assembly statistic	Value
No. contigs	115,719
No. contigs > 1 kb	19,511
Assembly size (Mb)	96.74
Mean contig length (bp)	836
Median contig length (bp)	341
Max contig length (bp)	132,566
GC content	42.58
N_{50} (bp)	3292
L_{50} (bp)	6526
BUSCO completeness (%)	92.2
BUSCO fragmented (%)	0.8
BUSCO missing (%)	7.0

3.2. Summary statistics of the transcriptome assembly and annotation

Sequencing of the 21 libraries yielded a total of 751,578,474 150-bp paired-end reads. After trimming to remove any adapter contamination or low quality reads, an average of 35.4 ± 5.8 million reads remained per library. FastQC reports of the trimmed reads from all libraries showed high sequence quality (scores > 30) with limited adapter contamination or presence of overrepresented sequences. The transcriptome generated by the NCGAS pipeline was 96.74 megabases (Mb) with 115,719 contigs, a N50 of 3292 bp, and a GC content of 42.58% (Table 2). The BUSCO analysis that used metazoan as the single-copy ortholog reference showed high transcriptome completeness with a complete BUSCO score of 92.2% (Table 2). Therefore, this transcriptome should offer a suitable foundation for transcriptomic analyses of *M. franciscanus*.

The gene discovery and functional annotation analyses identified 35,632 contigs that blasted to known proteins in the public databases (Table S1). From these, 24,900 contigs were linked to GO classifications. Hypothetical or predicted proteins in these databases were excluded by discarding matches associated to “hypothetical”, “predicted”, “unknown” and “putative” categories. Over 95% of the annotated contigs hit against the genomes of the purple sea urchin, *Strongylocentrotus pupuratus*, followed by the sea star, *Acanthaster planci*, and the sea cucumber, *Apostichopus japonicus*. The functional annotation analysis retrieved 48,990 GO terms, with 23,053 linked to molecular function (mainly protein binding), 15,754 linked to biological process (mainly G protein-coupled receptor signaling pathway, oxidation-reduction process and transmembrane transport), and 10,183 linked to cellular component (mainly integral component of membrane) (Table S2). Finally, the enzyme code annotation with KEGG mapping identified 1948 transcripts, which represented 433 enzymes in 122 unique pathways (Table 3 and Table S3). KEGG pathways included those related to purine metabolism, biosynthesis of antibiotics, T cell receptor signaling pathway, Th1 and Th2 cell differentiation, and ether lipid metabolism.

Table 3
Top 10 KEGG pathways in the transcriptome.

Pathway	Pathway ID	No. transcripts	No. enzymes
Purine metabolism	map00230	825	47
Thiamine metabolism	map00730	727	6
Drug metabolism – other enzymes	map00983	233	16
Biosynthesis of antibiotics	map01130	185	100
T cell receptor signaling pathway	map04660	132	2
Th1 and Th2 cell differentiation	map04658	129	1
Glutathione metabolism	map00480	76	13
Ether lipid metabolism	map00565	69	7
Cysteine and methionine metabolism	map00270	60	23
Sphingolipid metabolism	map00600	58	14

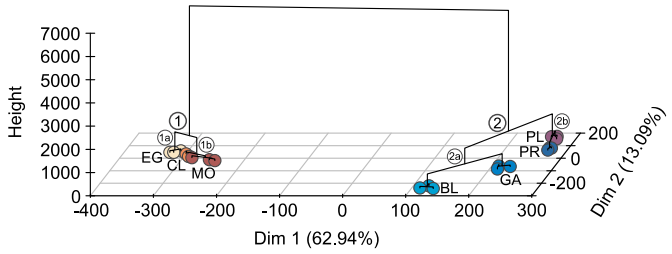

Fig. 1. PCA of *Mesocentrotus franciscanus* eggs and early developmental stages showing the first two dimensions and hierarchical clustering of the samples. Sample colors denote the different stages, which include: egg (EG), 8- to 16-cell (CL), morula (MO), blastula (BL), gastrula (GA), prism (PR), and pluteus (PL). Hierarchical clustering show two main clusters (1 and 2) that each contain two clusters (a and b).

3.3. Gene expression patterns in eggs and throughout early development

A total of 35,126 sequences remained after filtering to those with > 0.5 counts per million mapped reads across at least three of the 21 samples. A PCA of sample-to-sample distances showed that gene expression profiles were more similar within stages (i.e., among sample replicates) than across developmental stages (Fig. 1). The first and second dimensions captured 62.94% and 13.09% of the variation, respectively, and revealed a clear separation between egg/early embryonic stages and later developmental stages. Moreover, hierarchical clustering revealed two primary clusters (Fig. 1): cluster 1 included cluster 1a, which contained eggs (EG), and cluster 1b, which included the 8- to 16-cell (CL) and morula (MO) stages; cluster 2 included cluster 2a, which contained blastula (BL) and gastrula (GA) stages, and cluster 2b, which contained prism (PR) and pluteus stages (PL). In general, gene expression profiles followed the progression of development during which time major developmental processes and alterations in morphology occurred. Similar separations in transcriptomic patterns between earlier (e.g., egg and cleavage) and later (e.g., blastula and onwards) developmental stages have been observed in several other urchin species, and have been attributed to the transition between maternal and zygotic transcription (i.e., the MZT) (Gildor et al., 2016; Israel et al., 2016). The timing of the MZT in *M. franciscanus* will be discussed in further detail later (Section 3.4).

WGCNA was used to highlight groups of genes that were co-expressed in eggs and each developmental stage. After filtering, normalizing and voom-transforming the data, the remaining 35,126 genes were assigned into module eigengenes containing similarly expressed genes. Only 86 genes remained unclustered and unassigned, and were grouped into the grey module (Fig. 2). All other genes were assigned into 15 different modules that were designated by color, and hierarchical clustering of the module eigengenes revealed three main clusters (Fig. 2). Each module was related to developmental stage to generate eigengene networks with positive or negative correlation values ranging from 1 to −1 (Fig. 2).

Overall, WGCNA showed a mixed result for the 15 modules that were identified. Of the 15 module eigengenes, pink (908 genes) and green yellow (229 genes) were not significantly correlated to any stage (r^2 correlation ≤ 0.50, *p*-value ≥ .05). In addition, functional enrichment analyses did not identify any GO terms within the module eigengenes purple (294 genes), cyan (97 genes), magenta (340 genes), or midnight blue (55 genes). However, there were nine remaining module eigengenes that were significantly correlated to at least one stage (r^2 correlation ≥ 0.50 and *p*-value ≤ .05), and in which functional enrichment analyses successfully identified GO terms. These module eigengenes were tan (169 genes), brown (2912 genes), red (2166 genes), green (2613 genes), salmon (124 genes), yellow (2745 genes), black (1216 genes), turquoise (17,610 genes), and blue (3562 genes).

The WGCNA analysis revealed that the unfertilized eggs (EG) were significantly correlated to six module eigengenes, the greatest number of any developmental stage (Fig. 2). A significant negative correlation of EG with module eigengenes green, salmon, black, and turquoise revealed that, relative to the measured developmental stages post-fertilization, the egg transcriptome was characterized by a down-regulation of genes related to metabolic processes and catalytic activity (Table 4 and Table S4). Unfortunately, while EG had a significant positive correlation with module eigengenes purple and magenta, functional enrichment analyses failed to reveal any GO terms within these modules. However, in other studies, there is evidence that active transcription and translation occurs at low levels in unfertilized sea urchin eggs (Chassé et al., 2018; Ruderman and Schmidt, 1981). In the purple urchin, *Strongylocentrotus purpuratus*, eggs possess transcripts of genes related to the cell cycle and DNA replication (Tu et al., 2014). In the Mediterranean sea urchin, *Paracentrotus lividus,* genes related to the cell cycle and DNA replication are translated upon fertilization (i.e., at the one-cell embryo stage) (Chassé et al., 2018).

Unlike the eggs analyses, functional enrichment analyses were able to identify GO terms within module eigengenes positively correlated with early embryo stages. In this study, early embryo cell divisions are represented by the 8- to 16-cell stage (CL) and the morula stage (MO), whose transcriptomes are highly similar to one another (Fig. 1). CL and MO were both positively correlated to module eigengenes brown and green (module eigengene cluster 1, Fig. 2). The MO stage also had a significant correlation with module eigengene red (module eigengene cluster 1, Fig. 2). Enrichment analyses of these modules revealed that during these early cell divisions, the embryos contained transcripts encoding proteins related to metabolic processes, catalytic activity, and organelle and membrane formation (Table 4 and Table S4), which

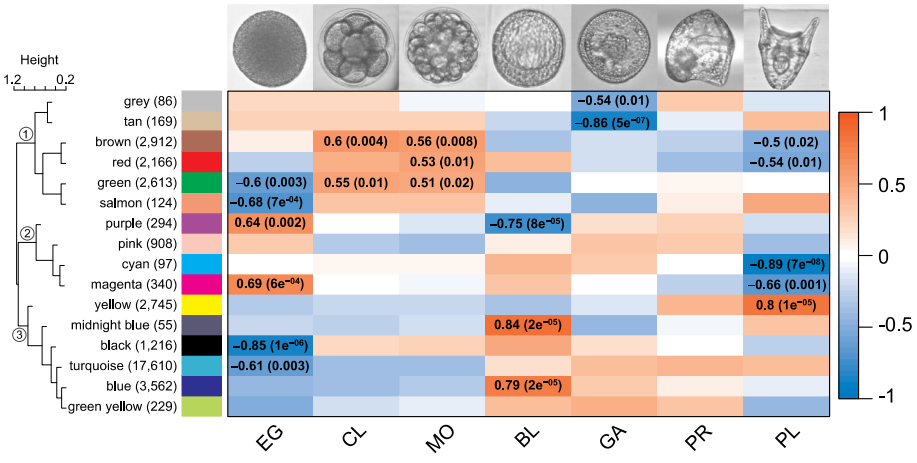

Fig. 2. WGCNA identified significant correlations between module eigengenes (rows) and stages (columns). The stages are: egg (EG), 8- to 16-cell (CL), morula (MO), blastula (BL), gastrula (GA), prism (PR), and pluteus (PL). The number of genes within each module eigengene is noted in parentheses following each color name. The red-blue color scale represents the strength of the correlation (1 to −1). Each correlation value (r^2) is followed by a *p*-value in parentheses. Hierarchical clustering of the module eigengenes revealed three primary clusters of gene expression (1–3). (For interpretation of the references to color in this figure legend, the reader is referred to the web version of this article.)

Table 4
Select GO term results from functional enrichment analyses of WGCNA module eigengenes.

GO ID	GO term name	GO category	FDR value	No. transcripts (% of ref)
Tan: GA ($r^2 = -0.86$)				
GO:0016021	Integral component of membrane	Cellular Component	6.67E-06	26 (0.6)
GO:0055114	oxidation-reduction process	Biological Process	2.27E-05	12 (1.2)
GO:0016491	Oxidoreductase activity	Molecular Function	2.82E-04	11 (1.1)
GO:0034220	Ion transmembrane transport	Biological Process	3.13E-03	6 (2)
GO:0015267	Channel activity	Molecular Function	5.97E-03	6 (1.7)
GO:0042623	ATPase activity, coupled	Molecular Function	5.97E-03	5 (2.5)
Brown: CL ($r^2 = 0.6$), MO ($r^2 = 0.56$), PL ($r^2 = -0.5$)				
GO:0016021	Integral component of membrane	Cellular Component	4.81E-12	207 (4.6)
GO:0005524	ATP binding	Molecular Function	1.63E-10	79 (6.5)
GO:0055085	Transmembrane transport	Biological Process	1.12E-05	57 (5.7)
GO:0007049	Cell cycle	Biological Process	5.60E-04	20 (8.5)
GO:0035556	Signal transduction	Biological Process	6.36E-04	24 (7.4)
GO:0140098	Catalytic activity, acting on RNA	Molecular Function	3.75E-03	20 (7.2)
Red: MO ($r^2 = 0.53$), PL ($r^2 = -0.54$)				
GO:0016021	Integral component of membrane	Cellular Component	9.33E-14	172 (3.8)
GO:0005524	ATP binding	Molecular Function	1.18E-11	68 (5.6)
GO:0022402	Cell cycle process	Biological Process	2.01E-05	16 (10.1)
GO:0007165	Signal transduction	Biological Process	3.78E-05	80 (3.5)
GO:0055114	Oxidation-reduction process	Biological Process	8.93E-04	39 (4.1)
GO:0055085	Transmembrane transport	Biological Process	2.53E-02	36 (3.5)
Green: EG ($r^2 = -0.6$), CL ($r^2 = 0.55$), MO ($r^2 = 0.51$)				
GO:0005524	ATP binding	Molecular Function	2.79E-34	117 (10)
GO:0035556	Intracellular signal transduction	Biological Process	2.35E-21	48 (16.1)
GO:0140098	Catalytic activity, acting on RNA	Molecular Function	1.48E-10	31 (11.7)
GO:0016021	Integral component of membrane	Cellular Component	4.84E-09	177 (3.9)
GO:0007049	Cell cycle	Biological Process	1.24E-08	26 (11.4)
GO:0055114	Oxidation-reduction process	Biological Process	5.06E-07	53 (5.7)
Salmon: EG ($r^2 = -0.68$)				
GO:0003824	Catalytic activity	Molecular Function	1.81E-07	34 (0.4)
GO:0005515	Protein binding	Molecular Function	9.29E-04	20 (0.4)
GO:0008152	Metabolic process	Biological Process	5.40E-03	26 (0.3)
GO:0008168	Methyltransferase activity	Molecular Function	5.40E-03	6 (1.7)
GO:0005543	Phospholipid binding	Molecular Function	5.40E-03	4 (4.7)
GO:0016020	Membrane	Cellular Component	9.21E-03	21 (0.3)
Yellow: PL ($r^2 = 0.8$)				
GO:0055114	Oxidation-reduction process	Biological Process	8.55E-23	87 (9.7)
GO:0005509	Calcium ion binding	Molecular Function	1.44E-16	77 (8.3)
GO:0022848	Acetylcholine-gated cation-selective channel activity	Molecular Function	1.78E-07	9 (60)
GO:0034220	Ion transmembrane transport	Biological Process	4.70E-07	27 (9.8)
GO:0005524	ATP binding	Molecular Function	3.95E-04	57 (4.6)
GO:0002376	Immune system process	Biological Process	6.06E-04	18 (8.4)
Black: EG ($r^2 = -0.85$)				
GO:0005515	Protein binding	Molecular Function	1.18E-11	111 (2.4)
GO:0003677	DNA binding	Molecular Function	8.07E-07	39 (3.3)
GO:0006464	Cellular protein modification process	Biological Process	3.49E-05	38 (2.8)
GO:0046872	Metal ion binding	Molecular Function	4.01E-05	69 (2.1)
GO:0006396	RNA processing	Biological Process	1.46E-04	16 (4.9)
GO:0016021	Integral component of membrane	Cellular Component	1.59E-04	86 (1.8)
Turquoise: EG ($r^2 = -0.61$)				
GO:0005524	ATP binding	Molecular Function	1.50E-92	499 (63.2)
GO:0015074	DNA integration	Biological Process	5.19E-40	271 (53.3)
GO:0005509	Calcium ion binding	Molecular Function	3.64E-36	315 (45.5)
GO:0003964	RNA-directed DNA polymerase activity	Molecular Function	3.09E-33	415 (38)
GO:0006278	RNA-dependent DNA biosynthetic process	Biological Process	4.22E-33	415 (37.9)
GO:0005525	GTP binding	Molecular Function	2.54E-19	136 (51.7)
Blue: BL ($r^2 = 0.79$)				
GO:0016021	Integral component of membrane	Cellular Component	7.53E-28	296 (6.7)
GO:0003964	RNA-directed DNA polymerase activity	Molecular Function	5.84E-24	132 (9.6)
GO:0005515	Protein binding	Molecular Function	5.01E-21	277 (6.1)
GO:0015074	DNA integration	Biological Process	1.28E-10	65 (9.1)
GO:0004672	Protein kinase activity	Molecular Function	2.26E-09	48 (10.3)
GO:0055085	Transmembrane transport	Biological Process	4.85E-06	67 (6.7)

likely reflect various processes involved in cell proliferation. This finding is consistent with proteomic data from early embryos of *S. purpuratus* (Guo et al., 2015). Additionally, GO terms related to signal transduction, G protein-coupled receptor signaling pathway, and transmembrane transport were identified. This result is similar to observations made in *P. lividus*, in which there was an enrichment of GO terms related to signaling pathways and cellular transport in the early embryological stages (Gildor et al., 2016). Lastly, GO terms related to the cell cycle were identified in each of the brown, green, and red modules. This is comparable to *S. purpuratus*, in which genes encoding

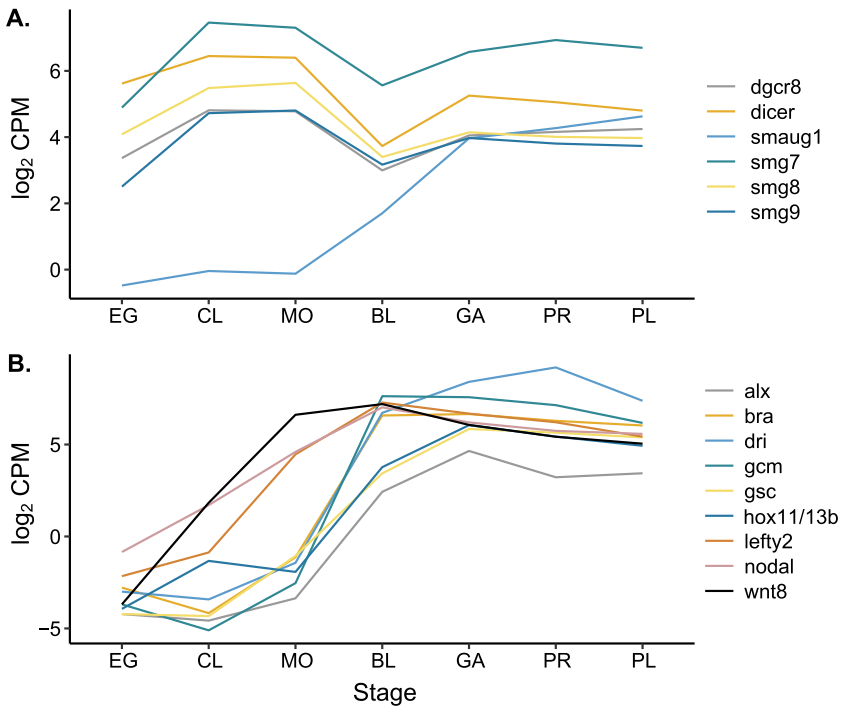

Fig. 3. The expression of putative genes that play a functional role during the MZT. These genes (A) regulate the removal of mRNA, and (B) regulate zygotic development. The data are in $\log_2$ counts per million reads ($\log_2$ CPM) expressed at each stage of development: egg (EG), 8- to 16-cell (CL), morula (MO), blastula (BL), gastrula (GA), prism (PR), and pluteus (PL).

proteins related to the cell cycle are prominent in cleavage stage embryos (Tu et al., 2014).

Upon progression to the blastula stage, extensive cell differentiation occurs in which the embryo forms a blastocoel, cilia, and enzymes required to digest the fertilization membrane during the hatching process (Barrett and Edwards, 1976; Lepage and Gache, 1989). With regard to stage-specific gene expression, the blastula stage (BL) was negatively correlated with module eigengene purple and positively correlated with module eigengenes midnight blue and blue (Fig. 2). Although functional enrichment analyses failed to reveal any GO terms within module eigengenes purple or midnight blue, module eigengene blue contained GO terms related to RNA-directed DNA polymerase activity, protein binding, DNA integration, G protein-coupled receptor activity, and transmembrane transport (Table 4 and Table S4). The enrichment of these genes is in alignment with other studies in which genes related to DNA replication and energy production were expressed during the blastula stage in *S. purpuratus* (Gildor et al., 2016; Tadros and Lipshitz, 2009).

Gastrulation is a major and fundamental process of metazoan development (Wolpert, 1992) that begins by invagination at the vegetal plate and the formation of the archenteron (Dan and Okazaki, 1956; Ettensohn, 1984). Somewhat surprisingly, there were few correlations between the gastrula stage (GA) and module eigengenes identified by WGCNA. GA was negatively correlated with only the module eigengene tan (module eigengene cluster 1, Fig. 2). GA was also negatively correlated with the grey module, which contained the unclustered and unassigned genes. Functional enrichment analysis of module eigengene tan revealed 39 GO terms, including oxidation-reduction process, integral component of membrane, ion transmembrane transport, and ATPase activity (Table 4 and Table S4). Unfortunately, the WGCNA did not identify any modules with a significant positive correlation with GA. Previous investigations of the *M. franciscanus* gastrula transcriptome, however, reported GO terms related to cell differentiation and signal transduction involved in cell cycle checkpoints (Gaitán-Espitia and Hofmann, 2017). In *S. purpuratus*, there is an increase in expression of genes related to biomineralization, the nervous system, immunity and the defensome once gastrulation begins (Tu et al., 2014).

The digestive tract and supporting skeletal rods are formed during the prism and early pluteus stages, which are necessary for the planktotrophic feeding strategy of the urchin larvae (Burke, 1980; Ettensohn and Malinda, 1993). The prism stage (PR) was not significantly correlated to any module eigengene (Fig. 2). However, its expression patterns were similar to that of the pluteus stage (PL) (Figs. 1 and 2). PL was negatively correlated to module eigengenes brown and red (module eigengene cluster 1, Fig. 2), which include GO terms related to ATP binding, integral component of membrane, transmembrane transport, signal transduction and the cell cycle (Table 4 and Table S4). PL was also negatively correlated with module eigengenes cyan and magenta, although functional enrichment analyses were unable to identify GO terms within these modules. Lastly, PL was positively correlated with one module eigenegene, yellow, which was within module eigengene cluster 3 (Fig. 2). Enrichment analysis identified GO terms within yellow that included those related to metallopeptidase activity, metabolism, adhesion, the cytoskeleton, and the immune system (Table 4 and Table S4). This observation was in agreement with our earlier work (Gaitán-Espitia and Hofmann, 2017), in which genes related to these processes and structures were up-regulated in *M. franciscanus* pluteus larvae relative to gastrula stage embryos. The yellow module also included GO terms related to ATP binding, oxidation-reduction process, calcium ion binding, acetylcholine-gated cation-selective channel activity, and ion transmembrane transport (Table 4 and Table S4). This expression pattern likely reflects the energy production and biomineralization processes necessary to support gut and skeletal formation in the developing pluteus larvae.

3.4. The maternal-to-zygotic transition

To examine the timing of the MZT, we assessed: (1) the decline of maternally-derived transcripts, and (2) the increase of zygotic transcription. Upon targeting genes that play a role in the degradation of maternal RNAs, one *DGCR8*-like gene (*dgcr8*), one *dicer* gene (*dicer*), one *smaug* homolog (*smaug1*) and three putative *smg* genes (*smg7*, *smg8*, and *smg9*) were identified within the *M. franciscanus* developmental transcriptome (Table 1). The expression levels of *dgcr8, dicer*, *smg7*, *smg8*, and *smg9* all peaked during the 8- to 16-cell (CL) and morula (MO) stages (Fig. 3A). The *dgcr8* gene plays a role in processing

microRNAs that are required for degrading mRNAs in mammals (Marlow, 2010; Wang et al., 2007). The Mediterranean sea urchin, *P. lividius*, exhibited a similar pattern of expression of *dgcr8* as reported here, in which there was a peak in expression within 8- and 16-cell embryos (Gildor et al., 2016). The authors attributed this observation to the role of *dgcr8* in degrading maternal mRNAs (Gildor et al., 2016). *Dicer* is involved in clearing maternal messages in zebrafish and mice (Giraldez et al., 2005; Marlow, 2010), and mutations in the *dicer* gene are known to alter and arrest embryonic development in some species (Murchison et al., 2007).

The *smg* genes code for proteins that function in nonsense-mediated mRNA decay (NMD) in a variety of organisms (Okada-Katsuhata et al., 2012; Pulak and Anderson, 1993; Yamashita et al., 2009). The NMD pathway detects and degrades mRNAs, and is often described as a surveillance pathway that serves as a quality-control mechanism to remove mRNAs with premature termination codons (Chang et al., 2007; Hentze and Kulozik, 1999). However, the NMD pathway also serves functional roles that shape gene expression and are important for differentiation and development (Lykke-Andersen and Jensen, 2015). Additionally, the NMD pathway has been shown to selectively degrade mRNA transcripts with longer 3′ UTRs, causing a relative enrichment of shorter 3′ UTR transcripts (Bao et al., 2016). In zebrafish embryos, 3′ UTR length affects the stability of maternal mRNAs because longer 3′ UTRs confer resistance to codon-mediated deadenylation, the first step required for mRNA decay (Mishima and Tomari, 2016). Therefore, the removal of long 3′ UTR transcripts via the NMD pathway may increase the relative proportion of short 3′ UTR transcripts available for deadenylation and decay during the CL and MO stages. Overall, the peak in expression of *dgcr8, dicer*, *smg7*, *smg8*, and *smg9* during the CL and MO stages supports that maternal mRNAs are degraded during this period of embryonic development.

In contrast to the expression of *dgcr8*, *dicer*, and *smg* genes, *smaug1* was not expressed until the blastula stage (Fig. 3A). The *smaug* gene is a transcriptional regulator known to bind to and target maternal RNAs for degradation in *Drosophila melanogaster* and is highly conserved across taxa (Tadros et al., 2007). It is therefore possible that degradation of maternal mRNAs is still ongoing at the blastula stage. This differs from observations in *S. purpuratus*, in which maternal degradation appears to end prior to the blastula stage (Tadros and Lipshitz, 2009; Wei et al., 2006). With the exception of *smaug1* expression, the degradation of maternal transcripts appears to primarily occur during the 8- to 16-cell (CL) and morula (MO) stages. This is additionally supported by the WGCNA analysis, which revealed genes related to catalytic activity acting on RNA in module eigengenes brown and green, both of which share significant, positive correlations with the CL and MO stages (Table 4).

Evidence of maternal transcript degradation was also reflected by a decrease in levels of maternal transcripts, which were represented by those expressed in unfertilized eggs (EG). A heatmap of the top 500 transcripts expressed in eggs revealed that expression of these transcripts began to decline at the 8- to 16-cell and morula stages (Fig. 4). By the blastula stage, the overall patterns of the maternal transcript levels had completely changed, with moderate retention of some maternal transcripts, although the majority had dramatically decreased. Most of these maternal transcripts continued to show low levels relative to the eggs during the remaining stages of development (i.e., gastrula through pluteus stages). Taken together, the degradation of maternal RNAs and the resulting reduction in expression of maternal transcripts began as early as the 8-cell stage, although it is possible that the process begins even sooner after fertilization at a stage prior to what was examined in this study (e.g., at the 2-cell or 4-cell stage). This result is similar to the timing of maternal mRNA degradation in *S. purpuratus*, in which maternal transcripts are destabilized by early cleavage stages (Tadros and Lipshitz, 2009; Tu et al., 2014; Wei et al., 2006).

To examine the timing of zygotic genome activation, nine putative genes important for zygotic development were identified within the *M. franciscanus* transcriptome (Table 1). Of these, *hox11/13b*, *lefty2*, *nodal*, and *wnt8* increased in expression between egg and the earliest measured developmental stage, the 8- to 16-cell stage (Fig. 3B). The expression levels of *wnt8*, *nodal*, and *lefty2* increased further during the morula stage before they plateaued and maintained relatively consistent levels of expression from the blastula stage through the remainder of development. This is somewhat similar to the expression patterns observed in *S. purpuratus*, in which many of the zygotic genes increased during cleavage stages and reached peak expression levels at the blastula stage (Tadros and Lipshitz, 2009, Tu et al., 2014, Wei et al., 2006). The *homeobox 11/13b* (*hox11/13b*) gene is one of the earliest transcription factors necessary for endoderm cell specification in echinoderms (Peter and Davidson, 2010). Similar transcriptional mechanisms may underlie both *left-right determination factor-2* (*lefty2*) and *nodal* expression, which function together to establish the oral-aboral embryonic axis (Adachi et al., 1999; Duboc et al., 2004; Duboc et al., 2008). Lastly, *wnt8* is required for endomesoderm development in sea urchins, including cell differentiation and gastrulation processes (Minokawa et al., 2005; Wikramanayake et al., 2004). In agreement with our results, in *S. purpuratus* expression of a *wnt8* homolog has been observed beginning at the 16-cell stage (Wikramanayake et al., 2004). The expression of these transcripts during the CL and MO stages support that the activation of zygotic transcription in *M. franciscanus* may occur as early as third cleavage.

The remaining five zygotic transcripts, *alx*, *bra*, *dri*, *gcm*, and *gsc* remained at low levels of expression until the blastula stage (BL), at which time most reached their peak levels of expression (Fig. 3B). The expression of these transcripts remained fairly consistent for the remainder of development. *Aristaless-like homeobox* (*alx*) expression has a role in primary mesenchyme cell formation, and acts as an early regulatory gene for skeletogenesis (Ettensohn et al., 2003; Ettensohn, 2009). *Brachyury* (*bra*) functions in gastrulation and endoderm development (Peterson et al., 1999; Rast et al., 2002). The *dead ringer* (*dri*) gene is required for normal embryological development and is highly conserved across taxa (Shandala et al., 1999), functioning in skeletogenesis and oral ectoderm formation in sea urchins (Amore et al., 2003). The *glial cells missing* (*gcm*) gene functions in endomesoderm specification, particularly those of pigment cells (Ransick et al., 2002; Ransick and Davidson, 2006). Lastly, in sea urchin embryos, *goosecoid* (*gsc*) plays a role in regulating cell specification along the animal-vegetal and oral-aboral axes (Angerer et al., 2001).

The expression patterns of *hox11/13b*, *lefty2*, *nodal*, and *wnt8* may represent a first wave of zygotic activation during CL and MO stages, while the expression patterns of *alx*, *bra*, *dri*, *gcm*, and *gsc* may represent a second wave of zygotic genome activation that occurs at the BL stage. This pattern of zygotic genome activation is very similar to that of *S. purpuratus*, in which there is a minor wave of zygotic transcription during early cell divisions of the embryo, followed by a major wave of zygotic transcription at the blastula stage (Tadros and Lipshitz, 2009; Wei et al., 2006). Further evidence of the timing of zygotic genome activation was supported by the appearance of transcripts not associated with the maternal transcriptome. A heatmap of transcripts that were not expressed in unfertilized eggs (i.e., transcripts that were not maternally-derived) showed that a moderate number of these transcripts began to be expressed by the 8- to 16-cell and morula stages (Fig. 4). This event may represent the first, minor wave of zygotic activation. The majority of the transcripts that were not present in eggs, however, were expressed by the blastula, gastrula, prism, and pluteus stages. Thus, the appearance of these transcripts at the blastula stage appear to represent the major wave of zygotic activation in *M. franciscanus* development.

Overall, the timing of the MZT in *M. franciscanus* appears to span from early cleavage through the blastula stage, in which (1) maternal degradation begins at or before the 8- to 16-cell stage and persists to the blastula stage, and (2) zygotic activation occurs as a minor wave at the 8- to 16-cell and morula stages and manifests as a major wave by the

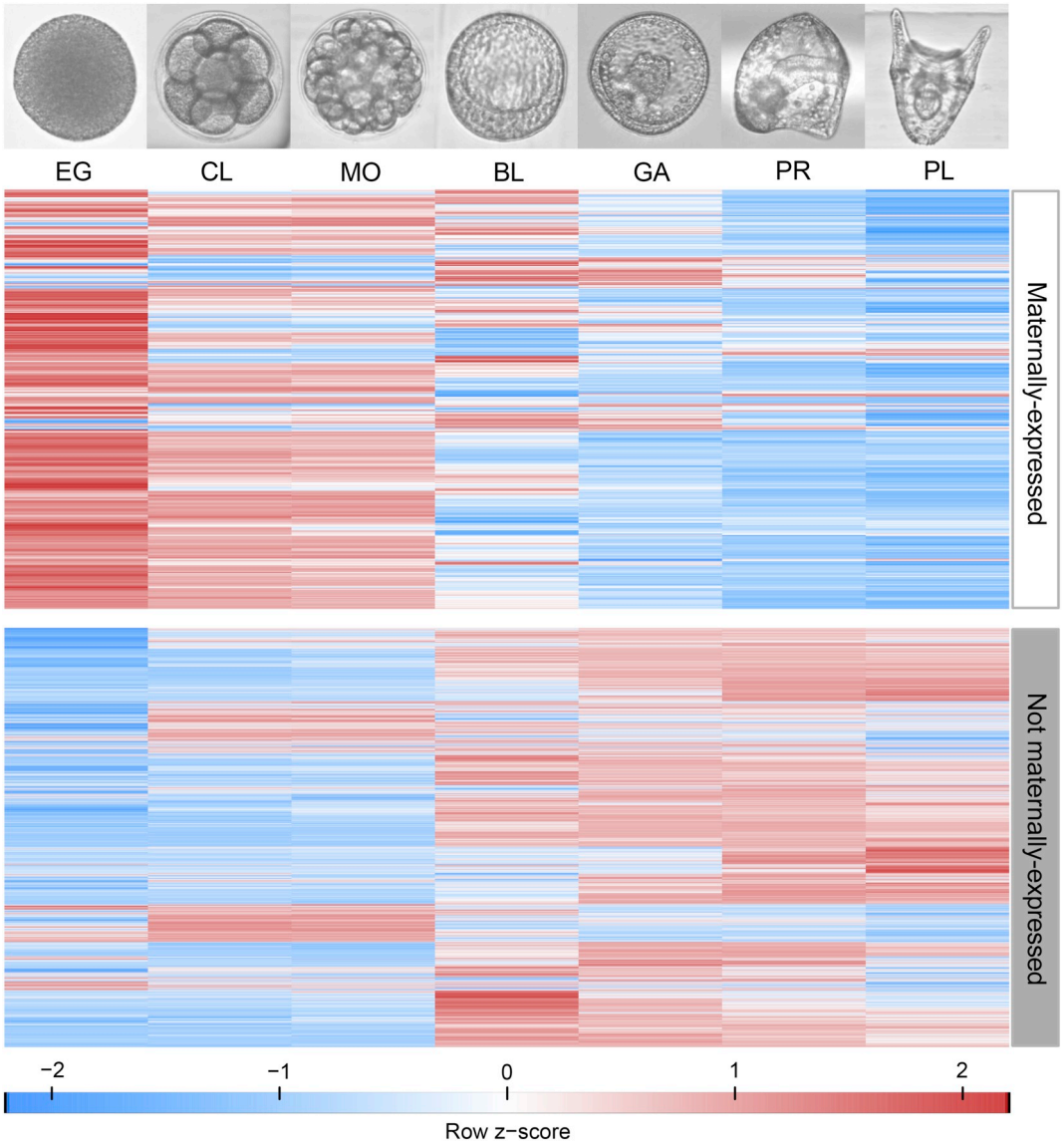

Fig. 4. Heatmaps of relative expression profiles for transcripts that are or are not maternally expressed. The rows are transcripts and the columns are in order of developmental stage: egg (EG), 8- to 16-cell (CL), morula (MO), blastula (BL), gastrula (GA), prism (PR), and pluteus (PL). Transcript expression data are in $\log_2$ counts per million reads ($\log_2$ CPM), and the data are scaled by row. The top heatmap contains the top 500 maternal transcripts expressed at EG (i.e., transcripts that are maternally expressed). The bottom heatmap contains 19,044 transcripts with a negative expression value of $\log_2$ CPM ($\log_2$ CPM < 0) at EG (i.e., transcripts that are not maternally expressed).

blastula stage. The occurrence of the MZT may partially explain the clear separation between egg/early embryonic stages (i.e., EG, CL, and MO) and later developmental stages (i.e., BL, GA, PR, and PL) evident in Fig. 1.

4. Conclusions

The transcriptome presented here is a useful molecular resource for studying *M. franciscanus*, a non-model organism and an important fishery species. We observed distinct patterns of gene expression across the eggs and early development of this sea urchin species, and identified periods of maternal RNA degradation and zygotic transcription. This genomic resource will support future investigations into the early development of *M. franciscanus*, and its response to environmental stress. In terms of developmental studies, the examination of the timing of the MZT will inform future gene expression studies that aim to target stages in which the zygotic transcriptome is fully activated. Lastly, these studies will facilitate our understanding of a marine species that has a significant ecological role in kelp forest ecosystems as a grazer, and is an economically valuable fishery species.

Data deposition

The raw sequence data and the *M. franciscanus* developmental transcriptome are available under NCBI Bioproject PRJNA531463 and Sequence Read Archive accession numbers SRR8866315–SRR8866335. The assembled transcriptome can be found in the NCBI Transcriptome Shotgun Assembly (TSA) database under accession GHJZ00000000. Additional data files including the transcriptome annotation can be found at https://doi.org/10.5281/zenodo.2649269.

Supplementary data to this article can be found online at https://doi.org/10.1016/j.margen.2019.05.007.

Declaration of interest

Declarations of interest: none.

Acknowledgments

The research was supported by a UC Climate Champion award to G.E.H. During this project, J.M.W. was supported by a UC Santa Barbara Regent's Fellowship and a U.S. National Science Foundation (NSF) Graduate Research Fellowship under Grant No. 1650114. This work used computing resources supported by NSF under grant No. ABI-1458641 to Indiana University. This work was also supported by resources from the Santa Barbara Coastal Long Term Ecological Research program (PI: Dr. Daniel Reed: NSF award OCE-1232779). The authors acknowledge the use of the UCSB and UCOP-supported Biological Nanostructures Laboratory within the California NanoSystems Institute. Specimens were collected in the Santa Barbara Channel under a California Scientific Collecting Permit to G.E.H. (SC-1223). The authors would like to thank Clint Nelson, Dr. Umihiko Hoshijima, Shannon Harrer, and Jordan Gallagher for their assistance in boating and diving operations while conducting sea urchin collections. The authors would like to thank Cailan Sugano and Margarita McInnis for their assistance during urchin spawning and culturing. The authors would also like to thank Sheri Sanders at the National Center for Genome Analysis and Support (NCGAS) at Indiana University for her assistance with bioinformatics associated with this project.

References

Adachi, H., Saijoh, Y., Mochida, K., Ohishi, S., Hashiguchi, H., Hirao, A., Hamada, H., 1999. Determination of left/right asymmetric expression of *nodal* by a left side-specific enhancer with sequence similarity to a *lefty-2* enhancer. Genes Dev. 13, 1589–1600.

Amore, G., Yavrouian, R.G., Peterson, K.J., Ransick, A., McClay, D.R., Davidson, E.H., 2003. *Spdeadringer*, a sea urchin embryo gene required separately in skeletogenic and oral ectoderm gene regulatory networks. Dev. Biol. 261, 55–81.

Andrew, N., Agatsuma, Y., Ballesteros, E., Bazhin, A., Creaser, E., Barnes, D., Botsford, L., Bradbury, A., Campbell, A.K., Dixon, J., Einarsson, S., Gerring, P., Hebert, K., Hunter, M., Hur, S., Johnson, C., Juinio-Meñez, P.E., Kalvass, R., Miller, C., Moreno, J., Palleiro, D., Rivas, S., Robinson, S.C., Schroeter, R., Steneck, R., Vadas, D., Woodby, Z. Xiaoqi, 2002. Status and management of world sea urchin fisheries. Oceanogr. Mar. Biol. 40, 343–425.

Andrews, S., 2010. FASTQC: A Quality Control Tool for High Throughput Sequence Data. Available online at. http://www.bioinformatics.babraham.ac.uk/projects/fastqc.

Angerer, L.M., Oleksyn, D.W., Levine, A.M., Li, X., Klein, W.H., Angerer, R.C., 2001. Sea urchin goosecoid function links fate specification along the animal-vegetal and oral-aboral embryonic axes. Development 128, 4393–4404.

Ashburner, M., Ball, C.A., Black, J.A., Botstein, D., Butler, H., Cherrry, J.M., Davis, A.P., Dolinski, K., Dwight, S.S., Eppig, J.T., Harris, M.A., Hill, D.P., Issel-Tarver, L., Kasarskis, A., Lewis, S., Matese, J.C., Richardson, J.E., Ringwald, M., Rubin, G.M., Sherlock, G., 2000. Gene ontology: tool for the unification of biology. Nat. Genet. 25, 25–29.

Bao, J., Vitting-Seerup, K., Waage, J., Tang, C., Ge, Y., Porse, B.T., Yan, W., 2016. UPF2-dependent nonsense-mediated mRNA decay pathway is essential for spermatogenesis by selectively eliminating longer 3'UTR transcripts. PLoS Genet. 12, e1005863. https://doi.org/10.1371/journal.pgen.1005863.

Barrett, D., Edwards, B.F., 1976. Hatching Enzyme of the Sea Urchin *Strongylocentrotus purpuratus*. Methods in Enzymology. Academic Press, pp. 354–373.

Bond, N.A., Cronin, M.F., Freeland, H., Mantua, N., 2015. Causes and impacts of the 2014 warm anomaly in the NE Pacific. Geophys. Res. Lett. 43, 3414–3420. https://doi.org/10.1002/2015GL063306.

Brekhman, V., Malik, A., Haas, B., Sher, N., Lotan, T., 2015. Transcriptome profiling of the dynamic life cycle of the scypohozoan jellyfish *Aurelia aurita*. BMC Genomics 16. https://doi.org/10.1186/s12864-015-1320-z.

Burke, R.D., 1980. Morphogenesis of the digestive tract of the pluteus larva of *Strongylocentrotus purpuratus*: shaping and bending. Int. J. Invertebr. Reprod. 2, 13–21. https://doi.org/10.1080/01651269.1980.10553338.

Byrne, M., 2011. Impact of ocean warming and ocean acidification on marine invertebrate life history stages: vulnerabilities and potential for persistence in a changing ocean. Oceanogr. Mar. Biol. 49, 1–42.

Byrne, M., 2012. Global change ecotoxicology: identification of early life history bottlenecks in marine invertebrates, variable species responses and variable experimental approaches. Mar. Environ. Res. 76, 3–15.

Byrne, M., Przeslawski, R., 2013. Multistressor impacts of warming and acidification of the ocean on marine invertebrates' life histories. Integr. Comp. Biol. 53, 582–596. https://doi.org/10.1093/icb/ict049.

Carruthers, M., Yurchenko, A.A., Augley, J.J., Adams, C.E., Herzyk, P., Elmer, K.R., 2018. *De novo* transcriptome assembly, annotation and comparison of four ecological and evolutionary model salmonid fish species. BMC Genomics 19. https://doi.org/10.1186/s12864-017-4379-x.

Chan, F., Barth, J.A., Blanchette, C., Byrne, R.H., Chavez, F., Cheriton, O., Feely, R.A., Friederich, G., Gaylord, B., Gouhier, T., Hacker, S., Hill, T., Hofmann, G., McManus, M.A., Menge, B.A., Nielsen, K.J., Russell, A., Sanford, E., Sevadjian, J., Washburn, L., 2017. Persistent spatial structuring of coastal ocean acidification in the California current system. Sci. Rep. 7. https://doi.org/10.1038/s41598-017-02777-y.

Chang, Y.-F., Imam, J.S., Wilkinson, M.F., 2007. The nonsense-mediated decay RNA surveillance pathway. Annu. Rev. Biochem. 76, 51–74. https://doi.org/10.1146/annurev.biochem.76.050106.093909.

Chassé, H., Aubert, J., Boulben, S., Le Corguillé, G., Corre, E., Cormier, P., Morales, J., 2018. Translatome analysis at the egg-to-embryo transition in sea urchin. Nucleic Acids Res. 46, 4607–4621. https://doi.org/10.1093/nar/gky258.

Chen, X., Zeng, D., Chen, X., Xie, D., Zhao, Y., Yang, C., Li, Y., Ma, N., Li, M., Yang, Q., Liao, Z., Wang, H., 2013. Transcriptome analysis of *Litopenaeus vannamei* in response to white spot syndrome virus infection. PLoS One 8, e73218.

Coppe, A., Bortoluzzi, S., Murari, G., Marino, I.A.M., Zane, L., Papetti, C., 2012. Sequencing and characterization of striped venus transcriptome expand resources for clam fishery genetics. PLoS One 7, e44185.

Dan, K., Okazaki, K., 1956. Cyto-embryological studies of sea urchins. III. Role of the secondary mesenchyme cells in the formation of the primitive gut in sea urchin larvae. Biol. Bull. 110, 29–42.

De Wit, P., Palumbi, S., 2012. Transcriptome-wide polymorphisms of red abalone (*Haliotis rufescens*) reveal patterns of gene flow and local adaptation. Mol. Ecol. 22, 2884–2897.

Dickson, A.G., Millero, F.J., 1987. A comparison of the equilibrium constants for the dissociation of carbonic acid in seawater media. Deep. Sea Res. Part I Oceanogr. Res. Pap. 34, 1733–1743.

Dickson, A.G., Sabine, C.L., Christian, J.R., 2007a. SOP 6b. Determination of the pH of Seawater Using the Indicator Dye *m*-Cresol Purple. Ver. 3.01. Jan 28, 2009.

Dickson, A.G., Sabine, C.L., Christian, J.R., 2007b. SOP 3b. Determination of Total Alkalinity in Seawater Using an Open-Cell Titration. Ver. 3.01 2008.

Duboc, V., Röttinger, E., Besnardeau, L., Lepage, T., 2004. Nodal and BMP2/4 signaling organizes the oral-aboral axis of the sea urchin embryo. Dev. Cell 6, 397–410.

Duboc, V., Lapraz, F., Besnardeau, L., Lepage, T., 2008. Lefty acts as an essential modulator of nodal activity during sea urchin oral–aboral axis formation. Dev. Biol. 320, 49–59.

Dupont, S., Thorndyke, M., 2009. Impact of CO_2-driven ocean acidification on invertebrates early life-history – what we know, what we need to know and what we can do. Biogeosciences 6, 3109–3131.

Ebert, T.A., Dixon, J.D., Schroeter, S.C., Kalvass, P.E., Richmond, N.T., Bradbury, W.A., Woodby, D.A., 1999. Growth and mortality of red sea urchins *Strongylocentrotus franciscanus* across a latitudinal gradient. Mar. Ecol. Prog. Ser. 190, 189–209.

Ekblom, R., Galindo, J., 2011. Applications of next generation sequencing in molecular ecology of non-model organisms. Heredity 107, 1–15.

Ettensohn, C.A., 1984. Primary invagination of the vegetal plate during sea urchin gastrulation. Am. Zool. 24, 571–588.

Ettensohn, C.A., 2009. Lessons from a gene regulatory network: echinoderm skeletogenesis provides insights into evolution, plasticity and morphogenesis. Development 136, 11–21. https://doi.org/10.1242/dev.023564.

Ettensohn, C.A., Malinda, K.M., 1993. Size regulation and morphogenesis: a cellular analysis of skeletogenesis in the sea urchin embryo. Development 119, 155–167.

Ettensohn, C.A., Illies, M.R., Oliveri, P., De Jong, D.L., 2003. Alx1, a member of the Cart1/Alx3/Alx4 subfamily of paired-class homeodomain proteins, is an essential component of the gene network controlling skeletogenic fate specification in the sea urchin embryo. Development 130, 2917–2928. https://doi.org/10.1242/dev.00511.

Fangue, N.A., O'Donnell, M.J., Sewell, M.A., Matson, P.G., MacPherson, A.C., Hofmann, G.E., 2010. A laboratory-based, experimental system for the study of ocean acidification effects on marine invertebrate larvae. Limnol. Oceanogr. Methods 8, 441–452.

Franks, S.J., Hoffmann, A.A., 2012. Genetics of climate change adaptation. Annu. Rev. Genet. 46, 185–208. https://doi.org/10.1146/annurev-genet-110711-155511.

Frölicher, T.L., Laufkötter, C., 2018. Emerging risks from marine heat waves. Nat. Commun. 9. https://doi.org/10.1038/s41467-018-03163-6.

Gaitán-Espitia, J.D., Hofmann, G.E., 2017. Gene expression profiling during the embryo-to-larva transition in the giant red sea urchin *Mesocentrotus franciscanus*. Ecol. Evol. 7, 2798–2811.

Gaitán-Espitia, J.D., Sánchez, R., Bruning, P., Cárdenas, L., 2016. Functional insights into the testis transcriptome of the edible sea urchin *Loxechinus albus*. Sci. Rep. 6. https://doi.org/10.1038/srep36516.

Gentemann, C.L., Fewings, M.R., García-Reyes, M., 2017. Satellite Sea surface temperatures along the West Coast of the United States during the 2014–2016 Northeast Pacific marine heat wave. Geophys. Res. Lett. 44, 312–319. https://doi.org/10.1002/2016GL071039.

Ghaffari, N., Sanchez-Flores, A., Doan, R., Garcia-Orozco, K.D., Chen, P.L., Ochoa-Leyva, A., Lopez-Zavala, A.A., Carrasco, J.S., Hong, C., Brieba, L.G., Rudiño-Piñera, E., Blood, P.D., Sawyer, J.E., Johson, C.D., Dindot, S.V., Sotelo-Mundo, R.R., Criscitiello, M.F., 2014. Novel transcriptome assembly and improved annotation of the whiteleg shrimp (*Litopenaeus vannamei*), a dominant crustacean in global seafood mariculture. Sci. Rep. 4.

Gilbert, D., 2013. Gene-omes built from mRNA seq not genome DNA. In: 7th Annual Arthropod Genomics Symposium, Notre Dame.

Gildor, T., Malik, A., Sher, N., Avraham, L., Ben-Tabou de-Leon, S., 2016. Quantitative developmental transcriptomes of the Mediterranean Sea urchin *Paracentrotus lividus*. Mar. Genomics 25, 89–94. https://doi.org/10.1016/j.margen.2015.11.013.

Gillard, G.B., Garama, D.J., Brown, C.M., 2014. The transcriptome of the NZ endemic sea urchin Kina (*Evechinus chloroticus*). BMC Genomics 15.

Giraldez, A.J., Cinalli, R.M., Glasner, M.E., Enright, A.J., Thomson, J.M., Baskerville, S., Hammond, S.M., Bartel, D.P., Schier, A.F., 2005. MicroRNAs regulate brain morphogenesis in zebrafish. Science 308, 833–838. https://doi.org/10.1126/science.

1109020.
Gosselin, L., Qian, P.-Y., 1997. Juvenile mortality in benthic marine invertebrates. Mar. Ecol. Prog. Ser. 146, 265–282.
Grabherr, M.G., Haas, B.J., Yassour, M., Levin, J.Z., Thompson, D.A., Amit, I., Adiconis, X., Fan, L., Raychowdhury, R., Zeng, Q., Chen, Z., Mauceli, E., Hacohen, N., Gnirke, A., Rhind, N., di Palma, F., Birren, B.W., Nusbaum, C., Lindblad-Toh, K., Friedman, N., Regev, A., 2011. Trinity: reconstructing a full-length transcriptome without a genome from RNA-Seq data. Nat. Biotechnol. 29, 644–652. https://doi.org/10.1038/nbt.1883.
Guo, H., Garcia-Vedrenne, A.E., Isserlin, R., Lugowski, A., Morada, A., Sun, A., Miao, Y., Kuzmanov, U., Wan, C., Ma, H., Foltz, K., Mili, A., 2015. Phosphoproteomic network analysis in the sea urchin *Strongylocentrotus purpuratus* reveals new candidates in egg activation. Proteom. 15, 4080–4095. https://doi.org/10.1002/pmic.201500159.
Gurevich, A., Saveliev, V., Vyahhi, N., Tesler, G., 2013. QUAST: quality assessment tool for genome assemblies. Bioinformatics 29, 1072–1075.
Hentze, M.W., Kulozik, A.E., 1999. A perfect message: RNA surveillance and nonsense-mediated decay. Cell 96, 307–310.
Heyland, A., Vue, Z., Voolstra, C.R., Medina, M., Moroz, L.L., 2011. Developmental transcriptome of *Aplysia californica*. J. Exp. Zool. B. Mol. Dev. Evol. 113–134. https://doi.org/10.1002/jez.b.21383.
Hofmann, G., Washburn, L., 2015. SBC LTER: Ocean: Time-Series: Mid-water SeaFET and CO_2 System Chemistry at Mohawk Reef (MKO), Ongoing Since 2012-01-11. Santa Barbara Coastal LTER.
Hu, Z.-Z., Kumar, A., Jha, B., Zhu, J., Huang, B., 2017. Persistence and predictions of the remarkable warm anomaly in the northeastern Pacific Ocean during 2014–16. J. Clim. 30, 689–702. https://doi.org/10.1175/JCLI-D-16-0348.1.
Israel, J.W., Martik, M.L., Byrne, M., Raff, E.C., Raff, R.A., McClay, D.R., Wray, G.A., 2016. Comparative developmental transcriptomics reveals rewiring of a highly conserved gene regulatory network during a major life history switch in the sea urchin genus *Heliocidaris*. PLoS Biol. 14, e1002391. https://doi.org/10.1371/journal.pbio.1002391.
Ji, P., Liu, G., Xu, J., Wang, X., Li, J., Zhao, Z., Zhang, X., Zhang, Y., Xu, P., Sun, X., 2012. Characterization of common carp transcriptome: sequencing, *De Novo* assembly, annotation and comparative genomics. PLoS One 7, e35152.
Jo, J., Park, J., Lee, H.-G., Kern, E.M.A., Cheon, S., Jin, S., Park, J.-K., Cho, S.-J., Park, C., 2016. Comparative transcriptome analysis of three color variants of the sea cucumber *Apostichopus japonicus*. Mar. Genomics 28, 21–24.
Jones, P., Binns, D., Chang, H.-Y., Fraser, M., Li, W., McAnulla, C., McWilliam, H., Maslen, J., Mitchell, A., Nuka, G., Pesseat, S., Quinn, A.F., Sangrador-Vegas, A., Scheremetjew, M., Yong, S.-Y., Lopez, R., Hunter, S., 2014. InterProScan 5: genome-scale protein function classification. Bioinformatics 30, 1236–1240.
Kanehisa, M., Goto, S., 2000. KEGG: Kyoto Encyclopedia of genes and genomes. Nucleic Acids Res. 28, 27–30.
Keesing, J., Hall, K., 1998. Review of harvests and status of world sea urchin fisheries points to opportunities for aquaculture. J. Shellfish Res. 17, 1597–1604.
Krueger, F., 2015. Trim Galore!: A Wrapper Tool around Cutadapt and FastQC to Consistently Apply Quality and Adapter Trimming to FastQ Files. Available at: www.bioinformatics.babraham.ac.uk/projects/trim_galore/.
Kurihara, H., 2008. Effects of CO_2-driven ocean acidification on the early developmental stages of invertebrates. Mar. Ecol. Prog. Ser. 373.
Langfelder, P., Horvath, S., 2008. WGCNA: an R package for weighted correlation network analysis. Bmc Bioinform. 9. https://doi.org/10.1186/1471-2105-9-559.
Langmead, B., Salzberg, S.L., 2012. Fast gapped-read alignment with Bowtie 2. Nat. Methods 9, 357–359.
Le, S., Josse, J., Husson, F., 2008. FactoMineR: an R package for multivariate analysis. J. Stat. Softw. 25, 1–18.
Leighton, D., Jones, L., North, W., 1966. Ecological relationships between giant kelp and sea urchins in southern California. In: Young, E., Maclachlan, J. (Eds.), Proceedings of the 5th International Seaweed Symposium. Pergamon Press, pp. 141–153.
Lenz, P.H., Roncalli, V., Hassett, R.P., Wu, L.-S., Cieslack, M.C., Hartline, D.K., Christie, A.E., 2014. *De Novo* assembly of a transcriptome for *Calanus finmarchicus* (Crustacea, Copepoda) – the dominant zooplankter of the North Atlantic Ocean. PLoS One 9, e88589.
Lepage, T., Gache, C., 1989. Purification and characterization of the sea urchin embryo hatching enzyme. J. Biol. Chem. 264, 4787–4793.
Leung, J.Y.S., Connell, S.D., Russell, B.D., 2017. Heatwaves diminish the survival of a subtidal gastropod through reduction in energy budget and depletion of energy reserves. Sci. Rep. 7. https://doi.org/10.1038/s41598-017-16341-1.
Li, B., Dewey, C.N., 2011. RSEM: accurate transcript quantification from RNA-Seq data with or without a reference genome. BMC Bioinform. 12.
Liao, X., Cheng, L., Xu, P., Lu, G., Wachholtz, M., Sun, X., Chen, S., 2013. Transcriptome analysis of Crucian carp (*Carassius auratus*), an important aquaculture and hypoxia-tolerant species. PLoS One 8, e62308. https://doi.org/10.1371/journal.pone.0062308.
Lv, J., Liu, P., Gao, B., Wang, Y., Wang, Z., Chen, P., Li, J., 2014. Transcriptome analysis of the *Portunus trituberculatus*: De novo assembly, growth-related gene identification and marker discovery. PLoS One 9, e94055. https://doi.org/10.1371/journal.pone.0094055.
Lykke-Andersen, S., Jensen, T.H., 2015. Nonsense-mediated mRNA-decay: an intricate machinery that shapes transcriptomes. Nat. Rev. Mol. Cell Biol. 16, 665–677.
Marlow, F.L., 2010. Maternal Control of Development in Vertebrates. Morgan & Claypool Life Sciences.
Mehrbach, C., Culberson, C., Hawley, J., Pytkowicz, R., 1973. Measurement of the apparent dissociation constants of carbonic acid in seawater at atmospheric pressure. Limnol. Oceanogr. 18, 897–907.
Minokawa, T., Wikramanayake, A.H., Davidson, E.H., 2005. *cis*-Regulatory inputs of the *wnt8* gene in the sea urchin endomesoderm network. Dev. Biol. 288, 545–558.
Mishima, Y., Tomari, Y., 2016. Codon usage and 30 UTR length determine maternal mRNA stability in zebrafish. Mol. Cell 61, 874–885.
Murchison, E.P., Stein, P., Xuan, Z., Pan, H., Zhang, M.Q., Schultz, R.M., Hannon, G.J., 2007. Critical role for dicer in the female germline. Genes Dev. 21, 682–693.
Okada-Katsuhata, Y., Yamashita, A., Kutsuzawa, K., Izumi, N., Hirahara, F., Ohno, S., 2012. N- and C-terminal Upf1 phosphorylations create binding platforms for SMG-6 and SMG-5:SMG-7 during NMD. Nucleic Acids Res. 40, 1251–1266. https://doi.org/10.1093/nar/gkr791.
Oliver, E.C.J., Donat, M.G., Burrows, M.T., Moore, P.J., Smale, D.A., Alexander, L.V., Benthuysen, J.A., Feng, M., Gupta, A.S., Hobday, A.J., Holbrook, N.J., Perkins-Kirkpatrick, S.E., Scannell, H.A., Straub, S.C., Wernberg, T., 2018. Longer and more frequent marine heatwaves over the past century. Nat. Commun. 9. https://doi.org/10.1038/s41467-018-03732-9.
Peter, I.S., Davidson, E.H., 2010. The endoderm gene regulatory network in sea urchin embryos up to mid-blastula stage. Dev. Biol. 340, 188–199. https://doi.org/10.1016/j.ydbio.2009.10.037.
Peterson, K.J., Cameron, R.A., Tagawa, K., Satoh, N., Davidson, E.H., 1999. A comparative molecular approach to mesodermal patterning in basal deuterostomes: the expression pattern of *Brachyury* in the enteropneust hemichordate *Ptychodera flava*. Development 126, 85–95.
Pulak, R., Anderson, P., 1993. mRNA surveillance by the *Caenorhabditis elegans smg* genes. Genes Dev. 7, 1885–1897.
Ransick, A., Davidson, E.H., 2006. *cis*-regulatory processing of notch signaling input to the sea urchin *glial cells missing* gene during mesoderm specification. Dev. Biol. 297, 587–602.
Ransick, A., Rast, J.P., Minokawa, T., Calestani, C., Davidson, E.H., 2002. New early zygotic regulators expressed in endomesoderm of sea urchin embryos discovered by differential array hybridization. Dev. Biol. 246, 132–147. https://doi.org/10.1006/dbio.2002.0607.
Rast, J.P., Cameron, R.A., Poustka, A.J., Davidson, E.H., 2002. *brachyury* target genes in the early sea urchin embryo isolated by differential macroarray screening. Dev. Biol. 246, 191–208. https://doi.org/10.1006/dbio.2002.0654.
Reusch, T.B., Wood, T.E., 2007. Molecular ecology of global change. Mol. Ecol. 16, 3973–3992. https://doi.org/10.1111/j.1365-294X.2007.03454.x.
Ritchie, M., Phipson, B., Wu, D., Hu, Y., Law, C., Shi, W., Smyth, G., 2015. *limma* powers differential expression analyses for RNA-sequencing and microarray studies. Nucleic Acids Res. 43, e47.
Robbins, L., Hansen, M., Kleypas, J., Meylan, S., 2010. CO2calc—A user-friendly seawater carbon calculator for Windows, Max OS X, and iOS (iPhone). U.S. Geol. Surv. Open-File Rep. 17.
Robertson, G., Schein, J., Chiu, R., Corbett, R., Field, M., Jackman, S.D., Mungall, K., Lee, S., Okada, H.M., Qian, J.Q., Griffith, M., Raymond, A., Thiessen, N., Cezard, T., Butterfield, Y.S., Newsome, R., Chan, S.K., She, R., Varhol, R., Kamon, B., Prabhu, A.-L., Tam, A., Zhao, Y., Moore, R.A., Hirst, M., Marra, M.A., Jones, S.J.M., Hoodless, P.A., Birol, I., 2010. *De novo* assembly and analysis of RNA-seq data. Nat. Methods 7, 909–912.
Robinson, M.D., Oshlack, A., 2010. A scaling normalization method for differential expression analysis of RNA-seq data. Genome Biol. 11, R25.
Rogers-Bennett, L., 2007. The ecology of *Strongylocentrotus franciscanus* and *Strongylocentrotus purpuratus*. Dev. Aquac. Fish. Sci. 37, 393–425.
Rogers-Bennett, L., 2013. *Strongylocentrotus franciscanus* and *Strongylocentrotus purpuratus*. In: Lawrence, J.M. (Ed.), Sea Urchins: Biology and Ecology, pp. 413–435.
Ruderman, J.V., Schmidt, M.R., 1981. RNA transcription and translation in sea urchin oocytes and eggs. Dev. Biol. 81, 220–228. https://doi.org/10.1016/0012-1606(81)90285-2.
Sanford, E., Sones, J.L., García-Reyes, M., Goddard, J.H.R., 2019. Widespread shifts in the coastal biota of northern California during the 2014–2016 marine heatwaves. Sci. Rep. 9. https://doi.org/10.1038/s41598-019-40784-3.
Sato, K.N., Powell, J., Rudie, D., Levin, L.A., 2018. Evaluating the promise and pitfalls of a potential climate change–tolerant sea urchin fishery in southern California. ICES J. Mar. Sci. 75, 1029–1041. https://doi.org/10.1093/icesjms/fsx225.
Schulz, M.H., Zerbino, D.R., Vingron, M., Birney, E., 2012. *Oases*: robust *de novo* RNA-seq assembly across the dynamic range of expression levels. Bioinformatics 28, 1086–1092. https://doi.org/10.1093/bioinformatics/bts094.
Shandala, T., Kortschak, R.D., Gregory, S., Saint, R., 1999. The *Drosophila dead ringer* gene is required for early embryonic patterning through regulation of *argos* and *buttonhead* expression. Development 126, 4341–4349.
Shier, A.F., 2007. The maternal-zygotic transition: death and birth of RNAs. Science 316, 406–407. https://doi.org/10.1126/science.1140693.
Simão, F.A., Waterhouse, R.M., Ioannidis, P., Kriventseva, E.V., Zdobnov, E.M., 2015. BUSCO: assessing genome assembly and annotation completeness with single-copy orthologs. Bioinformatics 31, 3210–3212.
Souza, C.A., Murphy, N., Strugnell, J.M., 2018. De novo transcriptome assembly and functional annotation of the southern rock lobster (*Jasus edwardsii*). Mar. Genomics 42, 58–62.
Tadros, W., Lipshitz, H.D., 2009. The maternal-to-zygotic transition: a play in two acts. Development 136, 3033–3042. https://doi.org/10.1242/dev.033183.
Tadros, W., Goldman, A.L., Babak, T., Menzies, F., Orr-Weaver, T., Hughes, T.R., Westwood, J.T., Smibert, C.A., Lipshitz, H.D., 2007. SMAUG is a major regulator of maternal mRNA destabilization in *Drosophila* and its translation is activated by the PAN GU kinase. Dev. Cell 12, 143–155.
Tian, K., Lou, F., Gao, T., Zhou, Y., Miao, Z., Han, Z., 2018. *De novo* assembly and annotation of the whole transcriptome of *Sepiella maindroni*. Mar. Genomics 38, 13–16.
Tu, Q., Cameron, A., Davidson, E.H., 2014. Quantitative developmental transcriptomes of the sea urchin *Strongylocentrotus purpuratus*. Dev. Biol. 385, 160–167.

Valenzuela-Quiñonez, F., 2016. How fisheries management can benefit from genomics? Breif. Funct. Genom. 15, 352–357.
Wang, Y., Medvid, R., Melton, C., Jaenisch, R., Blelloch, R., 2007. DGCR8 is essential for microRNA biogenesis and silencing of embryonic stem cell self-renewal. Nat. Genet. 39, 380–385.
Wei, Z., Angerer, R., Angerer, L., 2006. A database of mRNA expression patterns for the sea urchin embryo. Dev. Biol. 300, 476–484. https://doi.org/10.1016/j.ydbio.2006.08.034.
Wenne, R., Boudry, P., Hemmer-Hansen, J., Lubieniecki, K.P., Was, A., Kause, A., 2007. What role for genomics in fisheries management and aquaculture? Aquat. Living Resour. 20, 241–255.
Wikramanayake, A.H., Peterson, R., Chen, J., Huang, L., Bince, J.M., McClay, D.R., Klein, W.H., 2004. Nuclear β-catenin-dependent Wnt8 signaling in vegetal cells of the early sea urchin embryo regulates gastrulation and differentiation of endoderm and mesodermal cell lineages. Genesis 39, 194–205.
Wolpert, L., 1992. Gastrulation and the evolution of development. Development 116, 7–13.
Xie, Y., Wu, G., Tang, J., Luo, R., Patterson, J., Liu, S., Huang, W., He, G., Gu, S., Li, S., Zhou, X., Lam, T.-W., Li, Y., Xu, X., Wong, G.K.-S., Wang, J., 2014. SOAPdenovo-trans: *de novo* transcriptome assembly with short RNA-Seq reads. Bioinformatics 30, 1660–1666.
Yamashita, A., Izumi, N., Kashima, I., Ohnishi, T., Saari, B., Katsuhata, Y., Muramatsu, R., Morita, T., Iwamatsu, A., Hachiya, T., Kurata, R., Hirano, H., Anderson, P., Ohno, S., 2009. SMG-8 and SMG-9, two novel subunits of the SMG-1 complex, regulate remodeling of the mRNA surveillance complex during nonsense-mediated mRNA decay. Genes Dev. 23, 1091–1105.
Zeng, V., Villanueva, K.E., Ewen-Campen, B.S., Alwes, F., Browne, W.E., Extavour, C.G., 2011. *De novo* assembly and characterization of a maternal and developmental transcriptome for the emerging model crustacean *Parhyale hawaiensis*. BMC Genomics 12. https://doi.org/10.1186/1471-2164-12-581.
Zerbino, D.R., Birney, E., 2008. Velvet: algorithms for de novo short read assembly using de Bruijn graphs. Genome Res. 18, 821–829.
Zhao, X., Yu, H., Kong, L., Li, Q., 2012. Transcriptomic responses to salinity stress in the Pacific oyster *Crassostrea gigas*. PLoS One 7, e46244.